OXFORD

SOT | Society of Toxicology
academic.oup.com/toxsci

TOXICOLOGICAL SCIENCES, 176(1), 2020, 137–146

doi: 10.1093/toxsci/kfaa050
Advance Access Publication Date: May 6, 2020
Research article

Systems Genetics and Systems Biology Analysis of Paraquat Neurotoxicity in BXD Recombinant Inbred Mice

Carolina Torres-Rojas,* Daming Zhuang,* Paola Jimenez-Carrion,* Isabel Silva,* James P. O'Callaghan,† Lu Lu,* Wenyuan Zhao,* Megan K. Mulligan,* Robert W. Williams,* and Byron C. Jones*,[1]

*Department of Genetics, Genomics, and Informatics, The University of Tennessee Health Science Center, Memphis, Tennessee 38163; and †Health Effects Laboratory Division, Centers for Disease Control and Prevention-NIOSH, Morgantown, West Virginia 26505

[1]To whom correspondence should be addressed at Department of Genetics, Genomics, and Informatics, The University of Tennessee Health Science Center, 71 South Manassas Street, Memphis, TN 38163. Fax: 901 448 1784. E-mail: bjone129@uthsc.edu.

ABSTRACT

Paraquat (PQ) is an herbicide used in many countries, including the United States. It is also implicated as a risk factor for sporadic Parkinson's disease, especially in those living in agricultural areas and drinking well water. Studies linking PQ to sporadic Parkinson's disease are not consistent however and there appears to be interindividual differential susceptibility. One likely reason is genetically based differential susceptibility to paraquat neurotoxicity in subpopulations. To address this issue, we tested the effects of paraquat in a genetic reference population of mice (the BXD recombinant inbred strain family). In our earlier work, we showed that in genetically susceptible mice, paraquat increases iron in the ventral midbrain, the area containing the substantia nigra. Our hypothesis is that genetic variability contributes to diverse PQ-related susceptibility and iron concentration. To test this hypothesis, we treated male mice from 28 to 39 BXD strains plus the parental strains with 1 of 3 doses of paraquat, 1, 5, and 10 mg/kg 3 times on a weekly basis. At the end of the treatment period, we analyzed the ventral midbrain for concentrations of iron, copper, and zinc, also we measured the concentration of paraquat in cerebellum, and proinflammatory cytokines in serum and cerebellum. The effect on paraquat-treated mice with 5 mg/kg and principal component analysis of iron showed suggestive quantitative trait loci on chromosome 5. Overall, our results suggest that gene *Prkag2* and related networks may serve as potential targets against paraquat toxicity and demonstrate the utility of genetically diverse mouse models for the study of complex human toxicity.

Key words: sporadic Parkinson's disease; systems genetics; recombinant inbred mice; cerebellum; ventral midbrain; metals.

Paraquat (1,1′-dimethyl-4,4′-bipyridinium dichloride, PQ) is an herbicide used in many parts of the world. It is also toxic to vertebrates and can cause pulmonary failure in humans who receive large doses (> 40 mg/kg). Long-term low-dose exposure is also suspected to be a risk factor for developing sporadic Parkinson's disease (sPD) (reviewed in Jones *et al.* [2014]). Agricultural workers are exposed to paraquat during handling, spraying, and those who live on farms using paraquat and drinking well water have an odds ratio of about 2 for developing sPD (Goldman *et al.*, 2012). Safe use of paraquat is problematic because workers may not have access to protective equipment, or the climate conditions are too severe, ie, hot and humid for wearing full protective clothing.

Paraquat targets dopaminergic neurons in the *substantia nigra pars compacta* (SNpc) (Jadavji *et al.*, 2019; Peng *et al.*, 2009; Yin *et al.*, 2011). Damage to these neurons constitutes the main pathophysiology underlying sPD; however, it appears that not all individuals are equally susceptible to developing PQ-related

sPD. It is likely that genetic factors play a role in host-based differential susceptibility. Indeed, Goldman *et al.* (2012) reported that individuals carrying the null mutant allele for glutathione S-transferase T are at greatly increased risk for PQ-related sPD. In earlier work, we showed that PQ disrupts iron regulation in the ventral midbrain (VMB) in mice susceptible to PQ-related damage of dopamine neurons in the SNpc (Yin *et al.*, 2011). Therefore, our hypothesis is that variable genetic factors contribute to differential paraquat-induced iron dyshomeostasis which causes neural toxicity by producing free oxygen radicals and by other mechanisms that need to be characterized. Our systems genetics approach in *ex vivo* experiments leads to a better description of the pathway and biology changes associated with paraquat exposure. Here, we report the effects of paraquat on concentration of iron, copper, and zinc in the VMB, distribution of paraquat to the cerebellum (CB) (as proxy tissue), *Il-1β* and *Lif* expression in cerebellum in the BXD recombinant inbred group, and proinflammatory cytokines quantification in serum in C57BL/6J (B6) and DBA/2J (D2), the parental lines for the BXD panel.

MATERIALS AND METHODS

Animals. Groups and group sizes were determined according to the methods showed in Jones and Mormède (2007). Ashbrook *et al.* (2019), recommend phenotyping 3–6 mice per strain when using the expanded BXD panel and demonstrate that for all levels of heritability it is preferable to maximize the number of genomes rather than the number of replicates to obtain power of mapping. Because initial studies of the parental B6 and D2 strains had shown no differences in the phenotype of male and female mice for the range of PQ concentrations used in the experiments reported here (Yin *et al.*, 2011), we reduced total mouse numbers by using all male mice, the average age of mice was 231.38 ± 18.66 days. For iron, copper, and zinc concentrations we used 3–6 mice per strain/treatment from 28 BXD recombinant inbred strains plus the parental B6 and D2 strains, for PQ in cerebellum we used 3–12 mice per strain/treatment from 39 BXD recombinant inbred strains plus the parental strains, for cytokine detection in serum we used the parental strains, for proinflammatory cytokine expression in cerebellum we used an average of 28 strains including the parental strains. All mice were obtained from the University of Tennessee Health Science Center (UTHSC) vivarium. The mice were maintained under a constant light-dark cycle (06:00–18:00, on-off rotation), ambient temperature was 21 ± 2°C, and humidity was 35%. The animals were fed Envigo diet 7912 containing 240 ppm Fe, 93 ppm Cu, and 63 ppm Zn, for 6 months. They also received tap water *ad libitum*; the water contained 1.6, 0.5, and 4.3 ppm Fe, Cu, and Zn, respectively. At 6 months of age, the mice were treated with paraquat dichloride trihydrate (PQ, product No. 36541, Sigma Chemicals, St. Louis, Missouri), the solutions were made fresh daily in saline and administered ip weekly for 3 weeks at 1 of 3 doses, 1, 5, and 10 mg/kg. Control mice were fed the same diet and injected (ip) with saline. All procedures were approved by the UTHSC Animal Care and Use Committee.

Procedure for metals quantification

- The animals were deeply anesthetized with isoflurane and decapitated. The brain was removed and dissected to yield the VMB and cerebellum.
- The VMB was weighed (mean of 21.7 ± 10 mg) and wet-ashed with nitric acid. Samples were then analyzed in a S2 PICOFOX instrument (Bruker, Berlin).
- Samples were irradiated for 500 s and the values for each element were normalized to tissue wet weights. Metal concentrations are reported as mean μg/g ± SEM by strain and PQ dose.
- Bioinformatic analysis of the difference between PQ-treated mice and control mice was performed using tools at www.genenetwork.org.

Procedure for paraquat quantification in cerebellum. The procedure follows that of Winnik *et al.* (2009) that uses an optimized microwave-assisted solvent extraction as a rapid and precise extraction method for PQ from mouse brain tissue. This extract was subsequently quantified by high-performance liquid chromatography followed by tandem mass spectrometric (LC-MS/MS) assay.

The cerebellum tissue was divided in half, weighed (mean of 24.53 ± 4.68 mg) and placed into a 1.5-ml microcentrifuge tube, containing 150 μl of 12% acetic acid with 20 ng/ml paraquat dichloride-(rings-d8) as internal standard (IS).

Centrifuge tubes were put into HP 500 (CEM Matthews, North Carolina) microwave vessels (5 per vessel) then extracted in a CEM Mars microwave oven for 30 min using 50% of 300 W power (parameters for 5 vessels). If more vessels were necessary, 5% power per additional vessel was added.

After extraction, both solid plus liquid phases were transferred to Microcon centrifuge filters with a membrane cut off at 10 kDa and were filtered using a refrigerated centrifuge (Thermo Scientific, Sorvall Legend Micro 21R Centrifuge, Germany) at 4°C and 14 000 × g for 90 min. Filtrates containing PQ were transferred into 1.5-ml tubes and stored at −20°C until analysis.

Standard solutions used to create the calibration curves were prepared by adding the appropriate amount of PQ solution to an extract of the biological matrix obtained by extraction of untreated brain tissue using the same microwave protocol as that for the treated samples Analytes from tissue extracts.

LC-MS/MS. This experiment was carried out on a Triple Quadrupole 4500/5500 Mass Spectrometer (SCIEX, Redwood City, California), equipped with Analyst (1.6.3) for data collection and MultiQuant (2.1) for quantitation analysis.

The SCIEX 4500 MS was coupled with a Nexera HPLC system with CBM20A Controller, 2 LC30AD pumps, CTO30A column oven (SHIMADZU, Columbia, Maryland). The autosampler is a PAL HTC-xt autosampler (CTC Analytics AG, Lake Elmo, Minnesota). The SCIEX 5500 MS was coupled with a Nexera XR HPLC system and SIL-20ACXR autosampler (SHIMADZU).

A Waters UPLC BEH HILIC column, 100 × 2.1 mm with 1.7 μm particle size, (WATERS, Milford, Massachusetts) was used for chromatographic separation. Mobile phase was composed of A, water, and B, methanol, both containing 5 mM ammonium formate and 0.05% formic acid (pH 3.5).

Isocratic elution at 40% B was used with a 4-min run time at a flow rate of 0.2 ml/min. There was an extra 0.5-min equilibration time before each injection. Injection volume was 10 μl.

For the MS/MS experiment, multiple reaction monitoring transitions were conducted at positive mode with an electrospray ionization source. The ion spray voltage was at 5.5 kV, and ion source temperature was set at 600°C. Gas1, gas2, and curtain gas were set at 60, 50, and 20, respectively. Collisionally activated dissociation gas was 7. Other analyte-specific parameters are summarized in Table 1.

Procedure for cytokine detection in serum. To quantify the concentration of proinflammatory cytokines in the serum, an electrochemiluminescence assay was performed using the Meso Scale

Table 1. Selected Multiple Reaction-monitoring Mode Parameters

Analyte	Transition (*m*/z)	T_R (min)	DP (V)	EP (V)	CE (V)	CXP (V)
Paraquat	185.1/170.1	1.68	70	10	23	6
Paraquat-d8 (IS)	193.1/178.1	1.53	78	10	30	5

Abbreviations: CE, collision energy; CXP, collision cell exit potential; DP, declustering potential; EP, entrance potential; IS, internal standard; T_R, retention time.

Discovery Quick Plex 120 instrument on samples of 50 µl of serum. This instrument uses a sandwich immunoassay method which captures the analyte in question with a precoated antibody and is later sealed with a detection antibody with an electro chemiluminescent tag. When a current is applied to the plate, a voltage is created, and the surface of the electrode causes this tag to emit light. The instrument then measures the light intensity and provides a quantitative measure of the analyte present in the sample (Meso Scale Discovery, MSD, 2017).

The protocol for the assay followed the guidelines of the MSD Cytokine Assay manual and used the antibodies, diluent, and calibrator provided by the company's kit:

- The calibrator was prepared using the lyophilized calibrator included in the kit (Calibrator 1) and adding 1000 µl of Diluent 41. The solution was reconstituted and inverted 3 times. After the solution was equilibrated at room temperature for 45 min, the standards were prepared using a 4-fold serial dilution to generate 7 calibrators.
- The frozen serum was left to thaw at room temperature for 2 h and then centrifuged. The samples were diluted with the Diluent 41 in a 2-fold dilution for interleukin 1 beta (IL-1β), interleukin 6 (IL-6), tumor necrosis factor alpha (TNF-α), and in a 4-fold dilution for monocyte chemoattractant protein 1(MCP-1).
- The detection antibody solution was prepared using the ×50 stock solution for each antibody and then adding the Diluent 45 provided by the kit to add up to 3000 µl. The wash buffer was prepared using 15 ml of the stock MSD Wash Buffer (×20) and 285 ml of deionized water. The read buffer was prepared using a 1:1 solution of the MSD Read Buffer T (×4) and deionized water.
- The microwell plate was washed 3 times with the MSD Wash Buffer and the samples were added. The plate was left to incubate shaking at room temperature for 2 h.
- After incubation, the plate was washed, and the prepared antibody solution was added. The plate was left to incubate at 2°C–8°C overnight.
- The plate was washed, and the Read Buffer T was added to each well. The plate was analyzed on the MSD instrument.

Procedure for proinflammatory cytokines expression in cerebellum. The cerebellum tissue was weighed (mean of 24.53 ± 4.68 mg). Samples were prepared and sent to the CDC/NIOSH Morgantown, WV 26505 (O'Callaghan's Lab) for real-time PCR. QIAGEN RNeasy Mini Kit 250 (Cat No./ID: 74106) for RNA isolation was used. For Reverse Transcription of RNA to cDNA for use in real-time PCR samples were prepared by adding 4 µg of RNA to RNase-free water for a total of 20 µl volume. Preparation of Master Mix 1 was done with 2 µl per sample of Oligo-dt primer (Thermo Fisher No. 18418012) and 2 µl per sample of dNTP mix (Thermo Fisher No. 18427088). Was prepared at least 10% excess volume to ensure sufficient quantity. Next, 4 µl of Master Mix 1 was added to each sample. Samples were incubated at 65°C for 10 min and placed on ice for 5 min and then quickly centrifuged. Master Mix 2 was prepared with 2 µl per sample of SuperScript III (Thermo Fisher No. 18080085), 2 µl per sample of RNase Out (Thermo Fisher No. 10777019), 8 µl per sample of 5 × first strand buffer (component of Thermo Fisher No. 18080085), and 4 µl per sample of DTT (component of Thermo Fisher No. 18080085). At least 10% excess volume was prepared to ensure sufficient quantity. Pipet 16 µl of Master Mix 2 per sample. Samples were incubated at 42°C for 2 h. Then, samples were incubated at 65°C for 5 min. Samples were chilled on ice; 160 µl of RNase-free water was added to samples. Storage was in −20°C freezer.

Real-time PCR (AB 7500) procedure. cDNA was prediluted from reverse transcription. If reverse transcription was 40 µl reaction, 160 µl of RNase-free water was added to the cDNA. If not, the following step must be done first. Prepare Master Mix (45 µl per sample) with the following: 17.5 µl RNase-free water, 2.5 µl of Taqman gene expression assay (Thermo Fisher No. 4331182—primer appropriate for gene of interest), 25 µl of Taqman Universal Master Mix (Thermo Fisher No. 4305719). Prepare at least 10% extra mix to ensure adequate volume; 5 µl of prediluted cDNA onto MicroAmp Optical 96-Well Reaction Plate (Thermo Fisher No. N8010560) was added; 45 µl of gene appropriate master mix onto Reaction Plate was added. Plate was covered with MicroAmp Optical 8 cap strips (Thermo Fisher No. 4323032). Caps were rolled tight with roller to ensure wells were all sealed . Assay was run in an Applied Biosystems 7500 with software V2.3. The following primers from Life Technologies were used, Gene (Catalog No., Assay ID): *Gapdh* as reference gene (4331182, Mm99999915_g1), *Tnf-α* (4331182, Mm00443258_m1), *Il-1β* (4331182 Mm01336189_m1), *Il-6* (4331182, Mm00446190_m1), *Lif* (4331182, Mm00434761_m1), *Osm* (4331182 Mm01193966_m1), *Ccl2* (4331182, Mm00441242_m1), *Gfap* (4331182, Mm01253033_m1).

Mapping quantitative trait loci. We used a web service for systems genetics called GeneNetwork (www.genenetwork.org, GN) (Mulligan *et al.*, 2017). We performed mapping using Genome-wide Efficient Mixed Model Association algorithm (Zhou and Stephens, 2012). Values of the BXD metal phenotypes in VMB were compared against ventral tegmental area (VTA) gene expression VCU BXD VTA Sal M430 2.0 (Jun09) RMA database, High Q Foundation (HQF) BXD Striatum ILM6.1 (Dec10v2) RankInv database, and HQF Striatum Affy Mouse Exon 1.0ST Gene Level (Dec09) RMA database. Also, we conducted quantitative trait loci (QTL) analysis for cerebellar PQ concentration, *Il-1β*, and *Lif* expression followed by correlations using the GenEx BXD Sal Cerebellum Affy M430 2.0 (Feb13) RMA males database. Principal component analysis (PCA) of the 3 phenotypes per metal in VMB, and PQ concentration in CB was done using GN, these PCA eigenvariables were saved as phenotypes in GN and were analyzed like other phenotypes. Single nucleotide polymorphisms (SNPs) count were retrieved from Sanger (https://www.sanger.ac.uk/sanger/Mouse_SnpViewer/rel-1303, last accessed April 20, 2020) using the release *REL-1303—GRCm38*.

Statistical analysis and calculation of gene expression fold change. All phenotypes measured were evaluated by analysis of variance (ANOVA) for a 2 between-subjects variables (strain, dose) experiment. We report means and standard errors of the mean by strain and dose. Heritability scores were calculated by ANOVA for each of the doses of paraquat singly by SS_{strain}/SS_{total} after Belknap (1998). Pairwise comparisons were done using Tukey's HSD. Main effects and interactions were considered statistically significant at $\alpha = .05$. Fold change was calculated using the

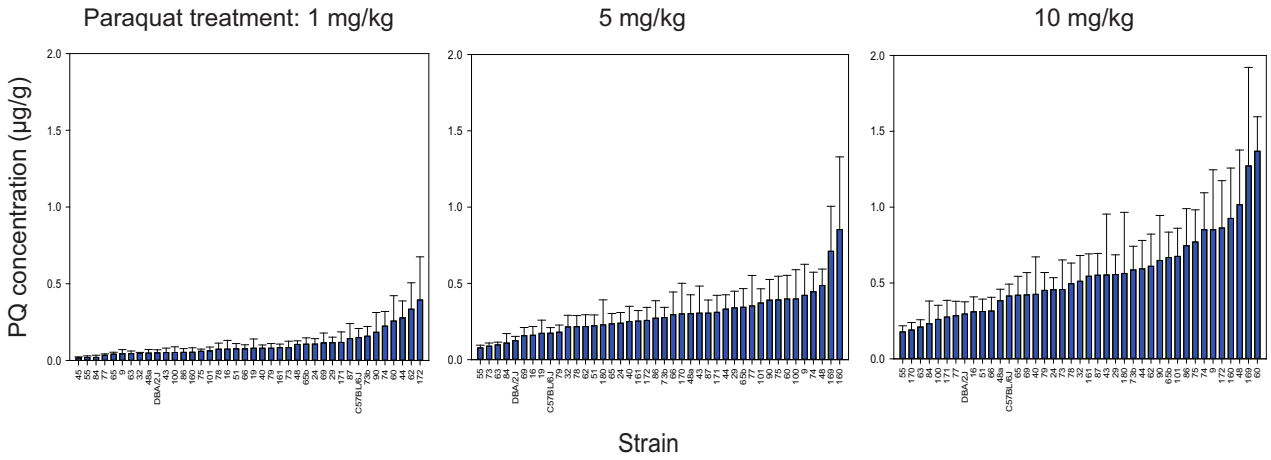

Figure 1. Strain distribution of paraquat concentration in cerebellum by strain and dose. Data are means and standard errors of paraquat (PQ)-treated mice. x-Axis lists the BXD strains. y-Axis shows means in µg/g tissue wet weight.

Table 2. Heritability Estimates for PQ Concentration in Cerebellum

	Trait	Heritability (h^2)
1	Paraquat concentration in cerebellum (µg/g) PQ 1 mg/kg	0.14
2	Paraquat concentration in cerebellum (µg/g) PQ 5 mg/kg	0.13
3	Paraquat concentration in cerebellum (µg/g) PQ 10 mg/kg	0.18

Table 3. Pearson (r) Product-Moment Correlations Among Paraquat Concentrations in Cerebellum

Trait1/Trait2 (PQ mg/kg)	5	10
1	.11, df = 37	.28, df = 36
5		.66*, df = 39

PQ doses: 1, 5, 10 (mg/kg).
*$p < .001$.

delta-delta cycle threshold method versus control [log2 fold change].

RESULTS

PQ Concentrations in Cerebellum by Dose

Because the measure of metals requires digestion of the tissues in nitric acid, we needed a proxy tissue for the VMB. Thus, previous work (Yin *et al.*, 2011) showed PQ can be detected in VMB and cerebellum of the parental strains B6 and D2 at similar concentrations by area, strain, and sex, after 3 weeks of exposure (5 mg/kg ip weekly injection). Here, we measured the pathway of variation through a considerable portion of the BXD panel under 3 different paraquat doses (Figure 1). We chose intraperitoneal route because the absorption of material delivered is typically slower and the pharmacokinetics of substances are similar to those observed after oral administration (Turner *et al.*, 2011).

From Figure 1, we can observe the individual variability of paraquat concentration in the cerebellum and its accumulation with dose. Some strains were not affected by treatment whereas others showed a tendency to accumulate paraquat with the dose. The quantitative analysis showed that strain and dose produced an effect on paraquat accumulation in the cerebellum $F_{(42,897)} = 2.15$, $p < .001$ and $F_{(2,897)} = 83.22$, $p < .001$, respectively. There was no effect of strain by treatment interaction ($F_{(78,897)} < 1$). Table 2 shows that trait variability due to genetic factors is around 15% for our model of paraquat concentration in cerebellum. Table 3 represents the relation among paraquat concentrations in cerebellum, there was no correlation between lower doses but higher doses (5 and 10 mg/kg) were correlated. This demonstrates 5 mg/kg dose is enough to see an effect of paraquat in this mouse model.

Effect of Paraquat on Proinflammatory Cytokines in Serum

We measured serum concentrations of IL-1β, IL-6, TNF-α, and MCP-1. Figures 2 and 3 represent the concentrations of proinflammatory cytokines in the serum from mice treated with different dosages of PQ (Saline or 0, 1, 5, and 10 [mg/kg]). For IL-1β (Figure 2A), ANOVA revealed mean effects for strain and treatment, and their interaction on IL-1β concentration in serum, $F_{(1,64)} = 28.214$, $p < .001$; $F_{(3,64)} = 7.115$, $p < .001$; $F_{(3,64)} = 5.329$, $p < .004$; respectively. For MCP-1 (Figure 2B) the analysis showed main effects for strain, treatment, and their interaction ($F_{(1,55)} = 8.941$, $p < .005$; $F_{(3,55)} = 7.702$, $p < .001$; $F_{(3,55)} = 5.092$, $p < .005$; respectively). These decreased serum IL-1β levels may indicate no peripheral systemic inflammatory responses.

In Figure 3A, we observed an increase in IL-6 with the maximum paraquat dosage of 10 mg/kg, although ANOVA revealed effect of strain $F_{(1,67)} = 7.443$, $p < .01$, but not of treatment and their interaction ($F_{(3,67)} = 1.079$, $p = .365$, $F_{(3,67)} < 1$, respectively). For TNF-α (Figure 3B) there were no effects of strain, treatment, nor their interaction ($F < 1$ for all).

Effect of Paraquat on Proinflammatory Cytokines Expression in Cerebellum

Here, we aimed at providing insight into the impact of paraquat exposure on brain inflammatory response. Microglia and astrocytes are the predominant immune cells in the central nervous system; microglia activation and astrogliosis, resulting from immune challenge or neuronal damage, are associated with interleukin IL-1β, IL-6 family, and other inflammatory molecule

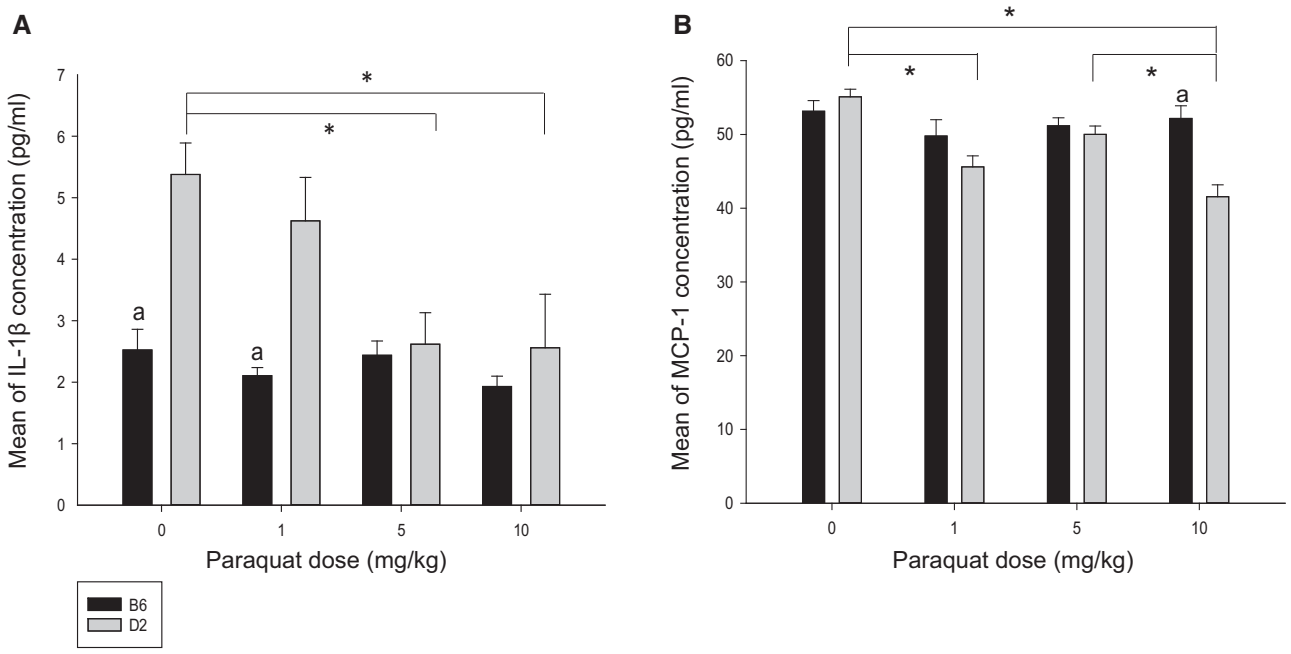

Figure 2. A, IL-1β levels in serum versus paraquat treatment in mg/kg, $^{*}p < .05$ in D2 by treatment, $^{a}p < .01$ B6 versus D2. B, Monocyte chemoattractant protein 1 (MCP-1) concentration in serum (pg/ml) versus paraquat treatment in mg/kg, $^{*}p < .01$ in D2 by treatment, $^{a}p < .01$ B6 versus D2 under PQ dose of 10 mg/kg. Black bars represent B6 and gray bars represent D2 mice.

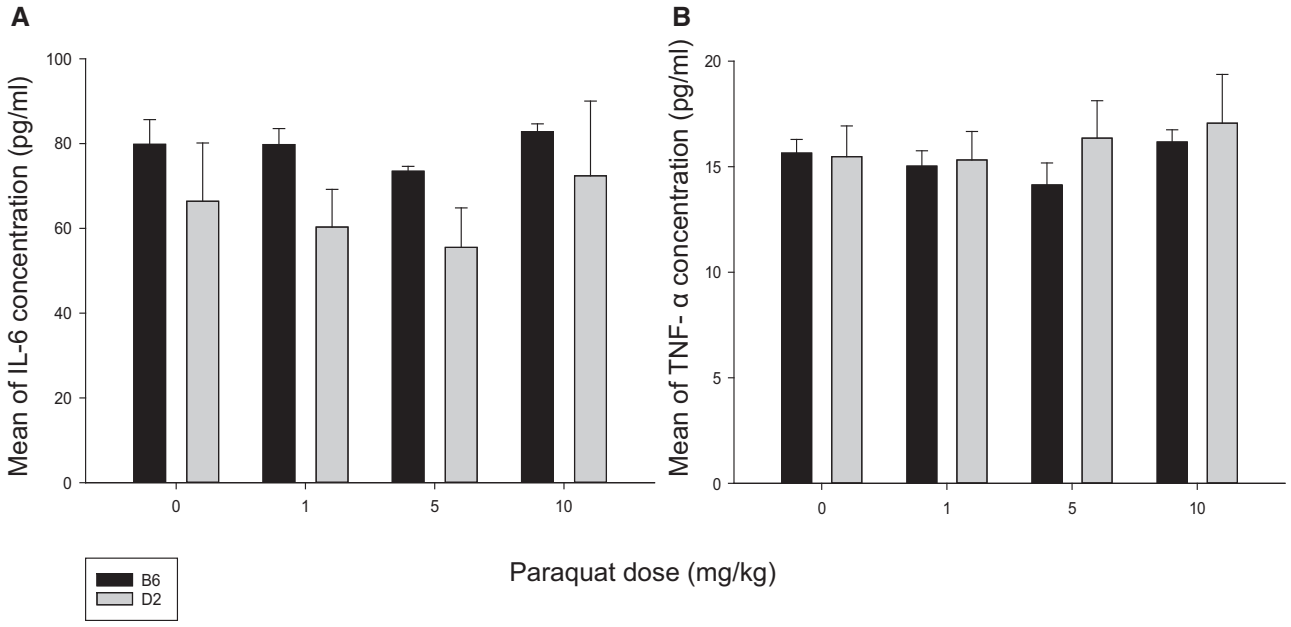

Figure 3. A, IL-6 level in serum versus paraquat treatment. B, Tumor necrosis factor alpha (TNF-α) in serum versus paraquat treatment. Black bars represent B6 and gray bars represent D2 mice. y-Axis values are expressed in pg/ml and x-axis values are expressed in mg/kg.

production (Farina *et al.*, 2007; Lampron *et al.*, 2013). From this fact and from our results in serum, we decided to measure mRNA expression of cytokines (*Il-1β*, *Lif*, *Osm*, *Ccl2*, and *Tnf-α*), and immune cytokine-producing cell markers (*Gfap*) in cerebellum after paraquat administration in mice. In this experiment, we used a cerebellum section from same groups of mice as for paraquat measurement in cerebellum. Groups have 71% the same strains among them. The results from rtPCR only showed detection of *Il-1β* and *Lif* in cerebellum (Figs. 4 and 5, respectively).

Interleukin 1 beta (*Il-1β*) is a proinflammatory cytokine essential to cellular defense and tissue repair, however, in brain this cytokine may have multiple functions like neuromodulation in healthy and also in pathogenic processes (reviewed in Hewett *et al.* [2012]). In Figure 4, we can see this cytokine is variable among strains ($F_{(43,280)} = 1.547$, $p < .03$). Also, we can see

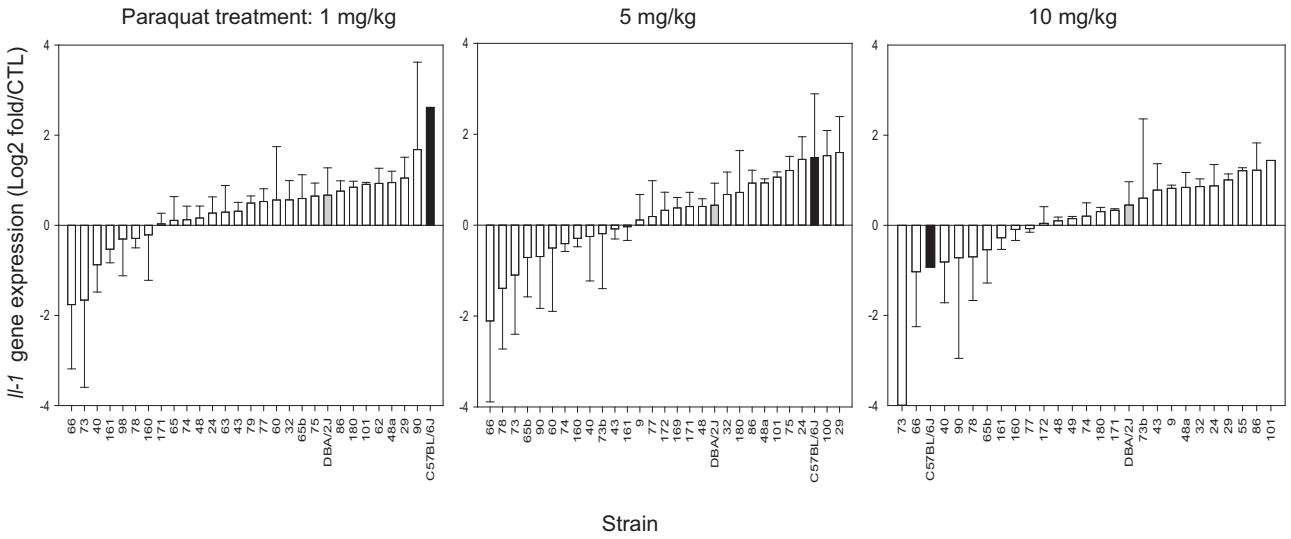

Figure 4. *Il-1β* gene expression in cerebellum by strain. Values are log2 fold versus control (CTL). Graphs from left to right are ordered by paraquat treatment (1, 5, 10 mg/kg).

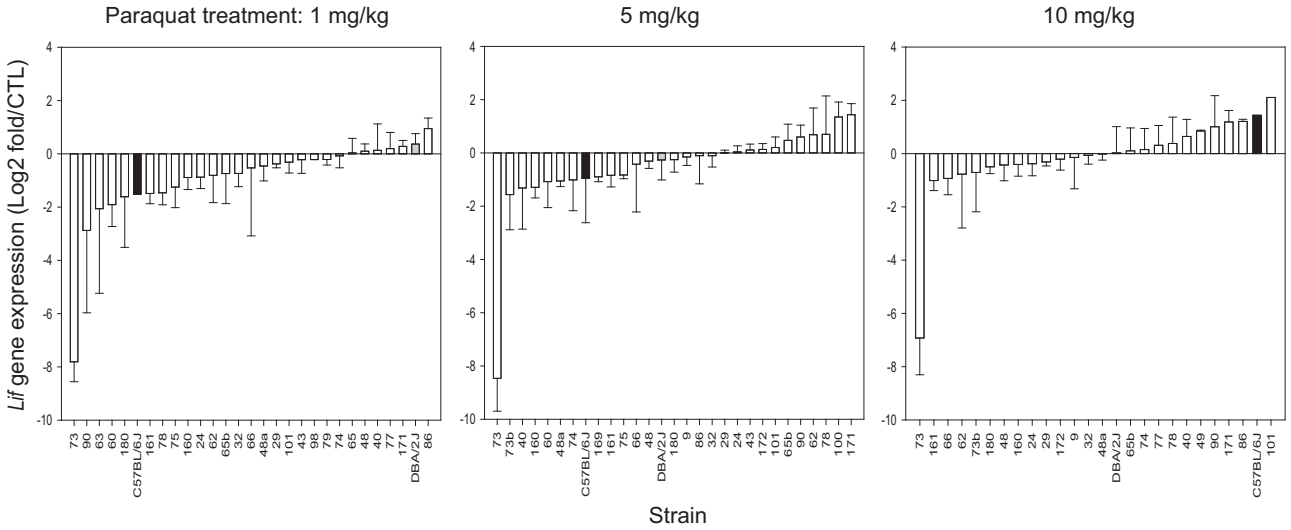

Figure 5. *Lif* gene expression in cerebellum by strain. Values are log2 fold versus control (CTL). Graphs from left to right are ordered by paraquat treatment (1, 5, 10 mg/kg).

that PQ treatment effect tended to reflect a reduction of *Il-1β* expression although ANOVA did not show treatment and strain × treatment effects ($F_{(2,280)} < 1$, $F_{(68,280)} < 1$, respectively). Leukemia inhibitory factor (*Lif*) belongs to IL-6 family and affects cell differentiation. Moreover, it can protect against amyloid β neurotoxicity (Lee *et al.*, 2019). From this experiment we observed high variability among strains in each of the treatments (Figure 5). From the analysis we obtained a main effect of strain $F_{(41,276)} = 6.268$, $p < .001$, but not for treatment and strain × treatment interaction $F_{(2,276)} = 2.622$, $p < .08$, $F_{(67,276)} < 1$, respectively.

Effect of Paraquat on Metal Concentrations in the Ventral Midbrain

Iron is an element essential for many neurological processes; however, in excess, iron is toxic to neurons (Gregory and Hayflick, 2013). Under normal conditions, iron is tightly regulated by a number of proteins that transport, sequester, and even change oxidation states. Paraquat has been shown to change oxidation states and produce reactive oxygen species (Peng *et al.*, 2009). These alterations may produce dysregulation of iron. Longer lifespans, genetic make-up, nutritional conditions, and environmental exposures are factors that affect the risk for iron-related neurodegeneration. Accordingly, our interest is the study of genetic-based individual differences in susceptibility to paraquat exposure and its effect on metal concentration in areas that have shown to be most affected under iron-related neurodegeneration such as the SNpc. Therefore, we measure not only iron but also copper and zinc. Each metal plays important roles in energy metabolism, neurotransmitter synthesis, myelination, and more. The roles of each metal in neurodegenerative diseases are well documented; however, less is known about how these metals interact under paraquat exposure. We measure these metal concentrations in

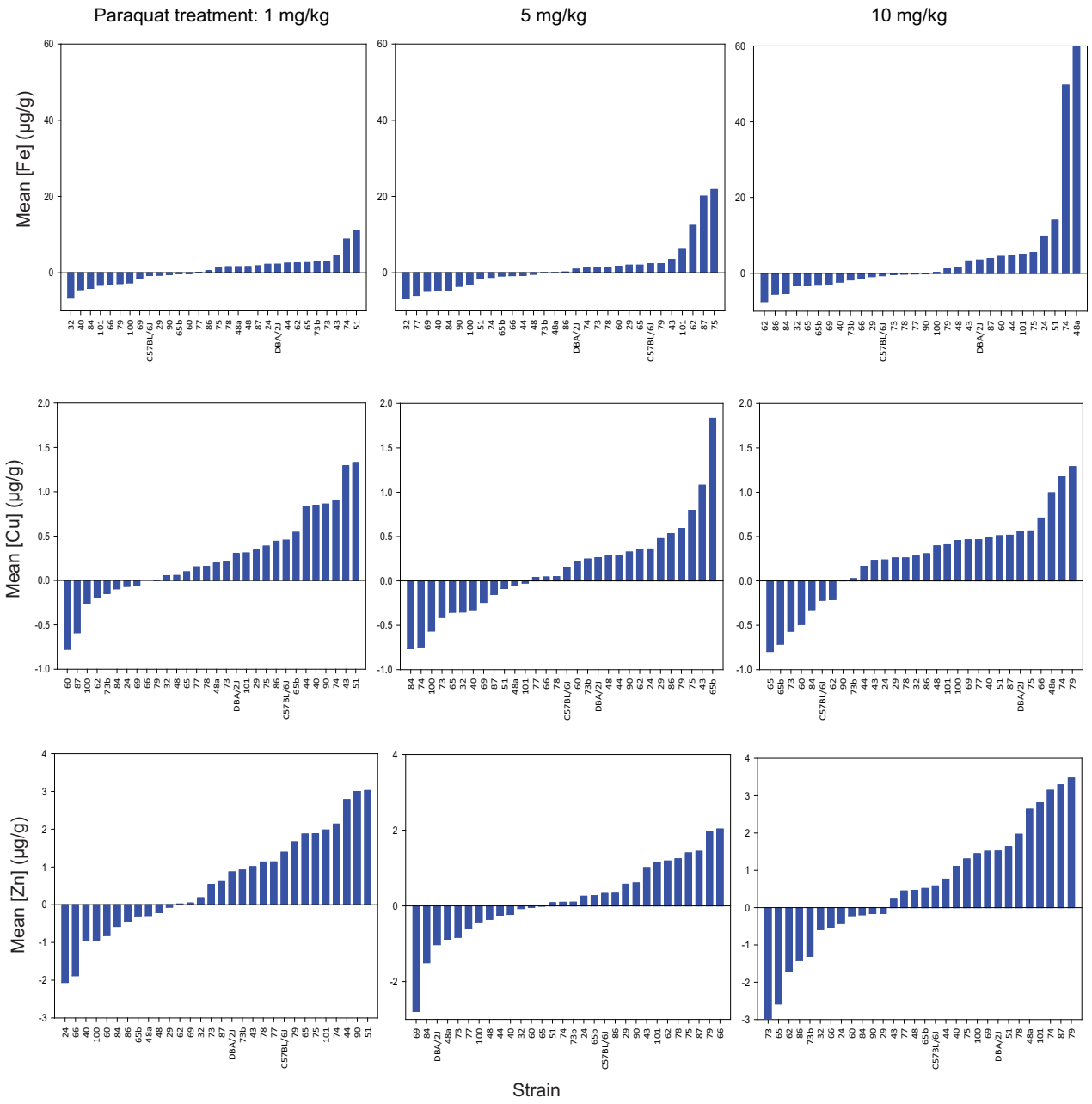

Figure 6. Metal concentrations by strain and dose. Data are differences between PQ-treated mice and control mice [µg/g]. x-Axis lists the strains. y-Axis shows mean differences in µg/g, tissue wet weight.

the VMB which contains the SNpc. The SNpc by itself is a very small tissue that is not feasible to use for total reflection x-ray fluorescence for trace analysis thus we dissected the VMB. Due to the nature of the experiment we used the whole VMB dissection to measure metals and no tissue left for measuring PQ in the VMB.

Also, to evaluate the influence of genetic background on phenotypes of metal concentration in VMB we selected a panel of 28 BXD recombinant inbred strains and 2 parental strains. We used 73% of the same strains that we used for measuring PQ in CB. We measured iron, copper, and zinc concentrations [Fe], [Cu], and [Zn], respectively as described in the Procedure section. We present the data as differences between treatment groups and control group (Figure 6). Some strains showed an increase in iron concentration with dosage, although not all strains show a consistent increase with the dosage. ANOVA revealed significant main effects of strain, PQ, and their interaction on [Fe] in the VMB $F_{(29,498)} = 1.783$, $p < .01$, $F_{(3,498)} = 2.811$, $p < .05$, $F_{(87,498)} = 1.565$, $p < .01$. For [Cu], ANOVA revealed a main effect of strain, $F_{(29,543)} = 6.859$, $p < .001$, but not for PQ nor strain × PQ interaction, $F_{(3,543)} = 2.257$, $p < .10$; $F_{(87,543)} < 1$, respectively. For [Zn], ANOVA showed a main effect for strain $F_{(29,554)} = 2.553$, $p < .001$, but not for PQ nor strain × PQ interaction $F_{(3,554)} = 1.311$, $p < .30$; $F_{(87,554)} < 1$, respectively.

Overall, the impact of paraquat treatment on iron concentration did show important variation depending on the specific

Table 4. Heritability Estimates for Phenotypic Traits in BXD Mouse

	Trait	Heritability (h^2)
1	Iron concentration in VMB (μg/g) saline	0.35
2	Iron concentration in VMB (μg/g) PQ 1 mg/kg	0.31
3	Iron concentration in VMB (μg/g) PQ 5 mg/kg	0.27
4	Iron concentration in VMB (μg/g) PQ 10 mg/kg	0.36

background strain evaluated, for example BXD101 showed a maintained increase in iron concentration with dosage. Heritability (h^2) estimates in Table 4 show how much is the genetic component underlying observed iron variability among strains.

The statistical analysis showed that iron is affected by treatment but not copper and zinc, however copper may be affected by iron because iron and copper concentrations are correlated under 10 mg/kg of PQ as we show in Table 5. Iron is correlated with zinc under 5 mg/kg treatment, and copper with zinc under 1 and 10 mg/kg doses (Table 5).

Genetic Mapping Identifies Intervals Associated With Paraquat Concentration and Metal Concentration in Young Adult Male Mice

Locally *cis*-regulated positional candidates are genes whose expression had a peak logarithm of the odds (LOD) at the location of the gene, are correlated with the phenotype, and have mean expression higher than 8, although this is limited to linear relations we do not discard there could be other genetic factors that may underlie the observed effects. Pearson's *r* correlations with *p* value are resumed in Table 6 and detailed in Supplementary Table 1. The SNP count is relative to C57BL/6J (Supplementary Table 1). We selected genes that have nonsynonymous variants because these variants may explain the variable effects of treatment and variable functionality in different regions.

To identify genes involved in paraquat effects on metal concentration, we analyzed iron, copper, and zinc concentrations within a cohort of adult male mice that model the genetic and phenotypic variation of human populations. Phenotypes, such as zinc concentration, are not shown in Table 6 because we did not observe suggestive QTL in the genetic mapping, any *cis*-regulated gene or genes correlated with the phenotype, therefore we did not nominate suggestive genes that we could relate to any effect of treatment. We also analyzed effects of PQ in CB and proinflammatory cytokine expression in CB.

From Table 6, we nominate *protein kinase, AMP-activated, gamma 2 noncatalytic subunit*, *Prkag2*. This gene has a nonsynonymous variant (missense variant, rs252553547) in exon 3 (A/G) and has a mean expression of 9.947 in VTA. This gene provides instructions for making 1 part (the gamma-2 subunit) of a larger enzyme called AMP-activated protein kinase. This enzyme senses and responds to energy demand within cells. Also, previous genetic analysis identified missense pathogenic variant (p.K290I) in this gene related to Wolff-Parkinson-White syndrome, ventricular hypertrophy due to glycogen accumulation, and conduction system disease (van der Steld *et al.*, 2017).

DISCUSSION

Whether PQ is a risk factor for sPD is not entirely settled. sPD is assigned to those cases where the subjects are about 50 years of age and beyond and it is generally believed that the etiology is related to the interaction between genes and environment. In contrast, PD occurring in younger individuals is much less common and more likely to be related primarily to genetics (Papapetropoulos *et al.*, 2007). Epidemiological studies on the topic are mixed and the animal models show differences as well.

Table 5. Significant Pearson (*r*) Product-Moment Correlations Among Metals by Dose

Trait1/Trait2	Cu	Zn
PQ = 1 mg/kg		
Cu		.521*, df = 28
PQ = 5 mg/kg		
Fe		.550*, df = 28
PQ = 10 mg/kg		
Fe	.505*, df = 28	
Cu		725*, df = 28

Correlations are based on differences between PQ-treated mice and controls.
*$p < .05$.

sPD is more prevalent in rural areas and this is most likely the result of gene-environment (exposure to agricultural chemicals) interactions. Previous studies linked paraquat exposure to Parkinson's disease (Pouchieu *et al.*, 2018). Industry argues that paraquat biodegrades and does not stay in water or crops in threatening concentrations to humans; however, others report that this compound is detectable in water (Fernández *et al.*, 1998; Hue *et al.*, 2018). This potentially is a concern for public health due to its wide use in agriculture and workers in contact with PQ can manifest its effects (Pouchieu *et al.*, 2018). Indeed, we have demonstrated that PQ can enter the brain.

We propose that disparities in PQ-related sPD likely stem from the possibility that there are genetic differences among individuals that confer differential susceptibility to paraquat neurotoxicity and that most epidemiological studies are too broad in inclusion of subjects to show this. One important epidemiological study that overcame this difficulty is that of Goldman *et al.* (2012). In this study, individuals who were identified as null mutants for the glutathione S-transferase theta-1 gene and exposed to paraquat through drinking well water on a farm were shown to be at more than 5 times at risk for developing sPD than those who were not mutant and exposed to paraquat.

Our study follows up on previous findings (Yin *et al.*, 2011) that when treated with PQ, B6 mice showed greater loss of tyrosine hydroxylase-positive neuronal staining in the substantia nigra, pars compacta than did D2 mice. Moreover, when tested for PQ-related gene expression differences, B6 mice showed far greater changes in gene expression than D2. When subjected to ontological analysis, the greater number of genes showing PQ-related changes in the B6 mice was iron-ion-binding protein genes. Subsequent work showed that PQ increased iron concentration in the VMB of B6 mice and not of D2 and that the increase was seen in the VMB but not the dorsal striatum. Here, we show that PQ alters iron concentration in the VMB with a significant PQ × strain interaction. No such interaction was observed for copper or zinc.

In this study time of exposure, sex, age, and diet were constant among groups, our observations were only dependent on dosage and strain. Metal and PQ concentrations were variable across the BXD family and heritability estimates that compare between-strain variance to within-strain variance demonstrate that part of this variability is attributable to genetic factors.

Genetic mapping of the phenotypes revealed significant QTL for iron (Chr 5 @ 24 Mb, LOD 4.09). We also mapped 8 suggestive QTLs for iron and copper, PQ in cerebellum, and *Il-1β* (Table 6 and Supplementary Table 1). From the significant QTL, we

Table 6. Locally *Cis*-regulated Positional Candidates

Record ID	QTL (Chr: Range Mb, [−log(*p*)], Max Peak Mb)	Correlation With Phenotype: Pearson's *r*, *p*(*r*)
21430	Chr2:93.3212–108.7769 Mb,	9630056G07Rik, $r = .54$, $< .02$
Diff Fe 1	3.26, 101.720448 Mb	*Mxd1*, $r = -.50$, $< .03$
	Chr6:76.542612–89.370565 Mb, 3.65, 88.577696 Mb	*Gftp1*, $r = -.54$, $< .02$
	Chr15: 12.687693–41.767064 Mb, 3.43, 14.271753 Mb	*Sdc2*, $r = -.86$, $< .004$
21413	Chr5: 21.026344–27.285288 Mb, 3.55, 24.3214 Mb	AB112350, $r = .54$, $< .02$
Diff Fe 5	Chr12: 116.685296–120.017431	*Nupl2*, $r = -.50$, $< .03$
	Mb, 3.01, 116.685296 Mb	*Abcb8*, $r = .57$, $< .02$
		Cdk5, $r = .57$, $< .02$
		Fastk, $r = .51$, $< .03$
		Prkag2, $r = .53$, $< .02$
		2900019A20Rik, $r = .58$, $< .02$
		1500035N22Rik, $r = .51$, $< .03$
		Arp, $r = -.57$, $< .02$
		Arp exon 13, $r = -.61$, $< .004$
		Zfp386, $r = -.51$, $< .03$
21414	Chr7: 89.123287–89.514184 Mb, 2.40, 89.123287 Mb	*Fzd4*, $r = -.85$, $< .02$
Diff Cu 1		*Picalm*, $r = .84$, $< .02$
21431	Chr1: 4.878037–15.981339 Mb, 3.18, 4.878037 Mb	*Terf1*, $r = .88$, $< .003$
Diff Cu 5	Chr2: 179.316875–181.990926 Mb, 2.74, 181.00898 Mb	*Kcnq2*, $r = .78$, $< .02$
	ChrX: 161.585623–164.079038 Mb, 2.64, 164.046333 Mb	*Rtel1*, $r = .78$, $< .02$
		Piga, $r = -.84$, $< .004$
21460	Chr1: 171.041085–178.015151Mb, 3.21, 171.041085 Mb	*Pvrl4*, $r = -.51$, $< .01$
PQ in CB 10		
21466	Chr5: 23.888018–25.891101 Mb, 4.09, 24.311463 Mb	*Arp3b*, $r = -.79$, $< .03$
PCA of Fe		***Prkag2***, $r = -.51$, $< .03$
		Fastk, $r = -.53$, $< .02$
21471	Chr7:134.8344–139.719Mb, 2.87, 134.834414 Mb	*Tcerg1l*, $r = -.82$, $< .03$
PCA of Cu		
21568	Chr9: 118–121.9159 Mb, 4.60, 119.286156 Mb	*Mobp*, −.542, $< .01$
Il-1b in CB PQ 5		*Rpl14*, .462, $< .03$
		Cyp8b1, −.559, $< .004$

Diff: difference between treatment group (PQ 1, 5, 10 mg/kg) and control. Genes whose expression had a peak LOD [−log(*p*)] at the location of the gene and were correlated with the phenotype were given higher priority. Pearson's *r* correlations with *p* value are reported.

nominate *Prkag2* as potential candidate gene for iron. Potential candidate gene is listed and bold for suggestive QTL in Table 6.

We subjected the significant and suggestive candidate genes from Table 6 to ontological analysis via String-db.org, when false discovery rate was $< .05$ the enriched functions for biological process consisted of:

- Regulation of telomeric loop disassembly
- Telomeric D-loop disassembly
- Dendrite morphogenesis.

Previous studies linked environmental/occupational exposure to pesticides with shorter telomere length (Andreotti *et al.*, 2015), and telomere attrition under different contaminants including pesticides (Louzon *et al.*, 2019). As consequence, telomere shortening can cause cellular apoptosis or senescence (Lin *et al.*, 2014). The effect on telomere structure and function implicates PQ as possibly accelerating neuronal aging.

Despite the apparent differences in findings both in humans and animal models, most researchers agree that sPD caused by PQ exposure or by other agents is a complex disease involving several biological systems. In our BXD murine family, we have shown strain (ie, genetic) differences in paraquat effects on divalent metal concentrations in the VMB, paraquat concentrations and dose-response in cerebellum (proxy for VMB), concentrations in serum and gene expression in cerebellum of proinflammatory cytokines. We assert therefore, that our animal model of multiple related inbred mouse strains (all were derived from multiple crossings of B6 and D2 inbred mice) is valuable to study the effect of toxicants in the central nervous system.

CONCLUSION

As we demonstrate here, paraquat can enter the brain and its effect on iron concentration is a result of strain × dose. Previous work showed that paraquat produces microglial activation within the substantia nigra (Jadavji *et al.*, 2019) and mediates microglial superoxide production that leads to iron-enhanced dopaminergic cell death *in vitro* (Peng *et al.*, 2009). Our results are consistent with but not conclusive that iron may indeed exacerbate paraquat neurotoxicity through complex pathways. Following on the nomination of candidate genes here we will investigate the role of PQ on specific telomere alterations and dendrite morphology. Our work here shows the heuristic value of systems genetics and systems biology approach in the complexity of neurotoxicology. Finally, the genetic variability in susceptibility to PQ-related changes in neurological parameters seen in our mouse model likely reflects the differential susceptibility to PQ neurotoxicity in humans.

SUPPLEMENTARY DATA

Supplementary data are available at *Toxicological Sciences* online.

ACKNOWLEDGMENTS

We thank Dr Ma Dejian from Pharmaceutical Sciences, UTHSC. We also thank our animal technician Melinda S. McCarty for taking care of our mice and helping us with the demographic data.

FUNDING

United States Public Health Service National Institute of Environmental Health Sciences (R01 ES022614). PQ quantification in CB was supported by the Office of the Director of the National Institutes of Health (S10OD016226).

DECLARATION OF CONFLICTING INTERESTS

The authors declared no potential conflicts of interest with respect to the research, authorship, and/or publication of this article.

REFERENCES

Andreotti, G., Hoppin, J. A., Hou, L., Koutros, S., Gadalla, S. M., Savage, S. A., Lubin, J., Blair, A., Hoxha, M., Baccarelli, A., *et al.* (2015). Pesticide use and relative leukocyte telomere length in the agricultural health study. *PLoS One* **10**, e0133382.

Ashbrook, D. G., Arends, D., Prins, P., Mulligan, M. K., Roy, S., Williams, E. G., Lutz, C. M., Valenzuela, A., Bohl, C. J., Ingels, J. F., *et al.* (2019). The expanded BXD family of mice: A cohort for experimental systems genetics and precision medicine. *bioRxiv*. doi:10.1101/672097.

Belknap, J. K. (1998). Effect of within-strain sample size on QTL detection and mapping using recombinant inbred mouse strains. *Behav. Genet.* **28**, 29–38.

Farina, C., Aloisi, F., and Meinl, E. (2007). Astrocytes are active players in cerebral innate immunity. *Trends Immunol.* **28**, 138–145.

Fernández, M., Ibáñez, M., Picó, Y., and Mañes, J. (1998). Spatial and temporal trends of paraquat, diquat, and difenzoquat contamination in water from marsh areas of the Valencian community (Spain). *Arch. Environ. Contam. Toxicol.* **35**, 377–384.

Goldman, S. M., Kamel, F., Ross, G. W., Bhudhikanok, G. S., Hoppin, J. A., Korell, M., Marras, C., Meng, C., Umbach, D. M., Kasten, M., *et al.* (2012). Genetic modification of the association of paraquat and Parkinson's disease. *Mov. Disord.* **27**, 1652–1658.

Gregory, A., and Hayflick, S, (2013). Neurodegeneration with brain iron accumulation disorders overview. In *GeneReviews®* (M. P. Adam, H. H. Ardinger, R. A. Pagon, S. E. Wallace, L. J. H. Bean, K. Stephens, A. Amemiya, Eds.) [Internet], pp. 1993–2020. University of Washington, Seattle, WA. https://www.ncbi.nlm.nih.gov/books/NBK121988/. Accessed April 20, 2020.

Hewett, S. J., Jackman, N. A., and Claycomb, R. J. (2012). Interleukin-1β in central nervous system injury and repair. *Eur. J. Neurodegener. Dis.* **1**, 195–211.

Hue, N. T., Nguyen, T. P. M., Nam, H., and Tung, N. H. (2018). Paraquat in surface water of some streams in Mai Chau Province, the Northern Vietnam: Concentrations, profiles, and human risk assessments. *J. Chem.* **2018**, 1–8.

Jadavji, N. M., Murray, L. K., Emmerson, J. T., Rudyk, C. A., Hayley, S., and Smith, P. D. (2019). Paraquat exposure increases oxidative stress within the dorsal striatum of male mice with a genetic deficiency in one-carbon metabolism. *Toxicol. Sci.* **169**, 25–33.

Jones, B. C., Huang, X., Mailman, R. B., Lu, L., and Williams, R. W. (2014). The perplexing paradox of paraquat: The case for host-based susceptibility and postulated neurodegenerative effects. *J. Biochem. Mol. Toxicol.* **28**, 191–197.

Jones, B. C., and Mormède, P. (2007). *Neurobehavioral Genetics: Methods and Applications*, pp. 31–42. CRC Press, Boca Raton, FL.

Lampron, A., Elali, A., and Rivest, S. (2013). Innate immunity in the CNS: Redefining the relationship between the CNS and its environment. *Neuron* **78**, 214–232.

Lee, H. J., Lee, J. O., Lee, Y. W., Kim, S. A., Seo, I. H., Han, J. A., Kang, M. J., Kim, S. J., Cho, Y. H., Park, J. J., *et al.* (2019). Lif, a novel myokine, protects against amyloid-beta-induced neurotoxicity via Akt-mediated autophagy signaling in hippocampal cells. *Int. J. Neuropsychopharmacol.* **22**, 402–414.

Lin, J., Kaur, P., Countryman, P., Opresko, P. L., and Wang, H. (2014). Unraveling secrets of telomeres: One molecule at a time. *DNA Repair* **20**, 142–153.

Louzon, M., Coeurdassier, M., Gimbert, F., Pauget, B., and Vaufleury, A. D. (2019). Telomere dynamic in humans and animals: Review and perspectives in environmental toxicology. *Environ. Int.* **131**, 105025.

Mulligan, M. K., Mozhui, K., Prins, P., and Williams, R. W. (2017). GeneNetwork: A toolbox for systems genetics. *Methods in Mol. Biol. (Clifton, N.J.)* **1488**, 75–120. doi:10.1007/978-1-4939-6427-7_4.

Papapetropoulos, S., Adi, N., Ellul, J., Argyriou, A. A., and Chroni, E. (2007). A prospective study of familial versus sporadic Parkinson's disease. *Neurodegener. Dis.* **4**, 424–427.

Peng, J., Stevenson, F. F., Oo, M. L., and Andersen, J. K. (2009). Iron-enhanced paraquat-mediated dopaminergic cell death due to increased oxidative stress as a consequence of microglial activation. *Free Radic. Biol. Med.* **46**, 312–320.

Pouchieu, C., Piel, C., Carles, C., Gruber, A., Helmer, C., Tual, S., Marcotullio, E., Lebailly, P., and Baldi, I. (2018). Pesticide use in agriculture and Parkinson's disease in the AGRICAN cohort study. *Int. J. Epidemiol.* **47**, 299–310.

Turner, P. V., Brabb, T., Pekow, C., and Vasbinder, M. A. (2011). Administration of substances to laboratory animals: Routes of administration and factors to consider. *J. Am. Assoc. Lab. Anim. Sci.* **50**, 600–613.

van der Steld, L. P., Campuzano, O., Pérez-Serra, A., Moura de Barros Zamorano, M., Sousa Matos, S., and Brugada, R. (2017). Wolff-Parkinson-White syndrome with ventricular hypertrophy in a Brazilian family. *Am. J. Case Rep.* **18**, 766–776.

Winnik, B., Barr, D. B., Thiruchelvam, M., Montesano, M. A., Richfield, E. K., and Buckley, B. (2009). Quantification of paraquat, MPTP, and MPP in brain tissue using microwave-assisted solvent extraction (MASE) and high-performance liquid chromatography-mass spectrometry. *Anal. Bioanal. Chem.* **395**, 195–201.

Yin, L., Lu, L., Prasad, K., Richfield, E. K., Unger, E. L., Xu, J., and Jones, B. C. (2011). Genetic-based, differential susceptibility to paraquat neurotoxicity in mice. *Neurotoxicol. Teratol.* **33**, 415–421.

Zhou, X., and Stephens, M. (2012). Genome-wide efficient mixed-model analysis for association studies. *Nat. Genet.* **44**, 821–824.